

# Enhanced thermal conductivity of TiO<sub>2</sub>—water based nanofluids

S.M.S. Murshed, K.C. Leong\*, C. Yang

*School of Mechanical and Aerospace Engineering, Nanyang Technological University, 50 Nanyang Avenue, Singapore 639798, Singapore*

Received 29 September 2004; accepted 7 December 2004

## Abstract

Nanofluids are prepared by dispersing TiO<sub>2</sub> nanoparticles in rod-shapes of  $\varnothing 10 \text{ nm} \times 40 \text{ nm}$  (diameter by length) and in spherical shapes of  $\varnothing 15 \text{ nm}$  in deionized water. A transient hot-wire apparatus with an integrated correlation model is used to measure the thermal conductivities of these nanofluids more conveniently. The pH value and viscosity of the nanofluids are also characterized. The experimental results show that the thermal conductivity increases with an increase of particle volume fraction. The particle size and shape also have effects on this enhancement of thermal conductivity. For TiO<sub>2</sub> particles of  $\varnothing 10 \text{ nm} \times 40 \text{ nm}$  and  $\varnothing 15 \text{ nm}$  dimensions with maximum 5% volume fraction, the enhancement is observed to be nearly 33% and close to 30%, respectively over the base fluid. For 5% volumetric loading of rod-shape TiO<sub>2</sub> nanoparticles of  $\varnothing 10 \text{ nm} \times 40 \text{ nm}$  in deionized water, this enhancement is found to be 12% higher than that predicted by the Hamilton–Crosser model [I & EC Fundamentals 1 (1962) 187]. However, with the same volumetric loading, the maximum enhancement is determined to be about 16% higher than that predicted by the Bruggeman model [Y. Ding, D. Wen, R.A. Williams, in: Proceedings of 6th International Symposium on Heat Transfer, Beijing, 2004, pp. 66–76] for TiO<sub>2</sub> nanoparticles of  $\varnothing 15 \text{ nm}$  in the same base fluid of deionized water. The measurement error is estimated to be within 2%.

© 2005 Elsevier SAS. All rights reserved.

*Keywords:* Nanoparticles; Nanofluids; Thermal conductivity; Hot-wire method

## 1. Introduction

Fluids with nanoparticles suspended in them are called nanofluids. This term was coined by Choi in 1995 at Argonne National Laboratory of USA [1]. Nanofluids are thought to be the next-generation heat transfer fluids, and they offer exciting possibilities due to their enhanced heat transfer performance compared to ordinary fluids. The advantages of these nanofluids are (1) better stability compared to those fluids containing micro- or milli-sized particles and (2) higher thermal conductive capability than the base fluids themselves. Nanofluids are proposed for various uses in important fields such as electronics, transportation, medical, and HVAC [2]. Hence, there is a need for fundamental understanding of the heat transfer behavior of nanofluids in order to exploit their potential benefits and applications.

Nanofluids with metallic nanoparticles and oxide nanoparticles have been investigated by several researchers [3] such as Choi [1], Das et al. [4], Xuan et al. [5], Eastman et al. [6, 7] and Lee et al. [8] who found great enhancement of thermal conductivity (5–60%) over the volume fraction range of 0.1–5%. In this study, TiO<sub>2</sub>—water based nanofluids are tested and their thermal conductivities are measured by the transient hot-wire method. The experimental results show a maximum 33% enhancement of thermal conductivity for 5% volumetric loading of nanoparticles. These results are also compared with theoretical predictions with several existing models.

## 2. Sample preparation and characterization

### 2.1. Sample preparation

A nanofluid does not mean a simple mixture of liquid and solid particles. To prepare nanofluids by suspending

\* Corresponding author. Tel.: +65 6790 5596, fax: +65 6792 2619.  
E-mail address: [mkleong@ntu.edu.sg](mailto:mkleong@ntu.edu.sg) (K.C. Leong).

### Nomenclature

$I$	current	A
$q$	heat rate	$\text{W}\cdot\text{m}^{-1}$
$L$	length of the wire	m
$R$	resistance	$\Omega$
$C_p$	specific heat	$\text{J}\cdot\text{kg}^{-1}\cdot\text{K}^{-1}$
$k$	thermal conductivity	$\text{W}\cdot\text{m}^{-1}\cdot\text{K}^{-1}$
$V$	voltage	V
$a$	wire radius	m
<i>Greek symbols</i>		
$\rho$	density	$\text{kg}\cdot\text{m}^{-3}$

$\gamma$	Euler constant	
$\theta$	temperature rise of the wire ( $T - T_0$ )	K
$\beta$	resistance temperature coefficient	$\text{K}^{-1}$
$\alpha$	thermal diffusivity	$\text{m}^2\cdot\text{s}^{-1}$
$\phi$	volume fraction	

### Subscripts

nf	nanofluid
w	wire
g	A/D converter
f	base fluid

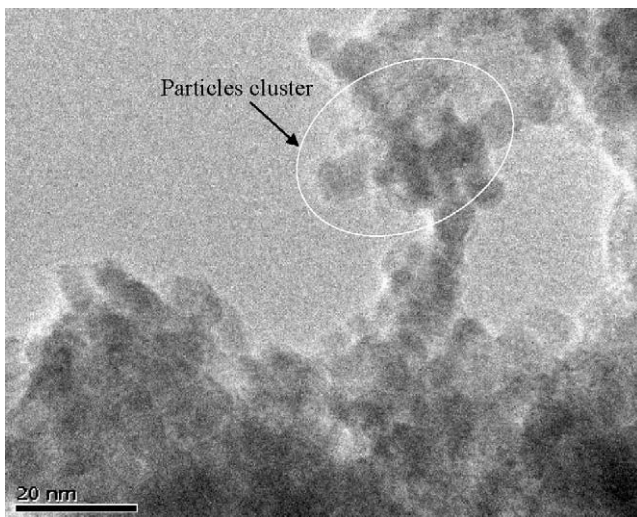


Fig. 1. TEM photograph of  $\varnothing 15$  nm  $\text{TiO}_2$  particles in deionized water.

nanoparticles into base fluids, proper mixing and stabilization of the particles are essential. Nanofluids dispersing copper, aluminum and their oxide nanoparticles have been widely investigated by many researchers [5–10]. However, titanium oxide, which has excellent chemical and physical stability, is not widely used although it is a cheap and commercially available mineral product. In this study, spherical-shape  $\text{TiO}_2$  nanoparticles of  $\varnothing 15$  nm and rod-shapes of  $\varnothing 10$  nm  $\times$  40 nm (Nanostructured and Amorphous Materials, Inc., USA) were used. Two types of sample nanofluids were prepared by dispersing  $\text{TiO}_2$  nanoparticles with different volume fractions in the deionized (DI) water base fluid. Their pH value, viscosity, and stability are characterized. An ultrasonic dismembrator was first used for nearly 8–10 hours to ensure proper mixtures of different volume fraction of  $\text{TiO}_2$  nanoparticles into the base fluid (DI water). A transmission electron microscope (TEM) and particle size analyzer were then used to monitor the dispersion, clustering and morphology of nanoparticles in base fluids, which are also considered as factors for higher heat transfer performance of nanofluids. The sizes of the nanoparticles in the base fluid were found to be larger than those specified by the

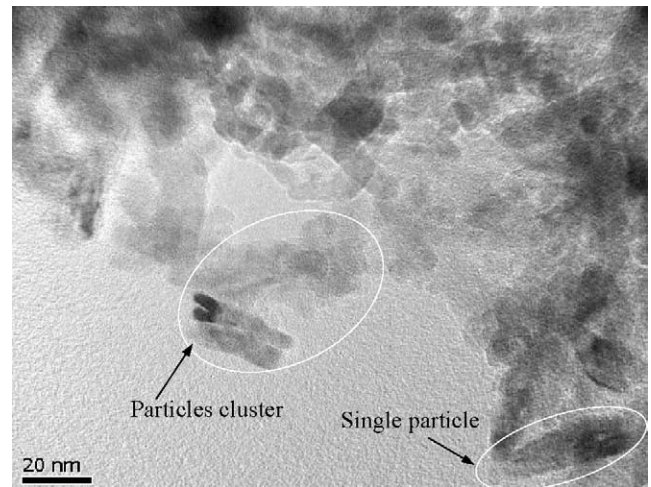


Fig. 2. TEM photograph of  $\varnothing 10$  nm  $\times$  40 nm  $\text{TiO}_2$  particles in deionized water.

supplier. This is because of the large particle density, huge number of particles, inter-particle attraction, and agglomeration of particles, which were observed using the particle size analyzer and TEM (Figs. 1 and 2). The particles are also not uniformly dispersed in the base fluid. There is therefore a need to use surfactants to break down the particle conglomeration in suspension. The surfactant keeps particles dispersed in base fluids by electrostatic repulsive forces among the particles and hydrophobic surface forces due to physical adsorption of surfactant in solution [11]. Oleic acid and cetyltrimethylammoniumbromide (CTAB) surfactants were used to ensure better stability and proper dispersion without affecting nanofluids' thermo-physical properties and single-phase heat transfer performance since the surfactant concentrations used in the experiments are very low (e.g., volume percentage around 0.01–0.02%). CTAB is found to be more effective.

### 2.2. Viscosity and pH value

The pH value and viscosity, which are considered as factors that may affect the stability of nanofluids were measured

at room temperature. For maximum 0.05 volume fraction of  $\text{TiO}_2$ — $\varnothing 10 \text{ nm} \times 40 \text{ nm}$  nanoparticles in deionized water, the viscosity was found to be  $1.55 \times 10^{-3} \text{ Pa.s}$ , which increases slightly with an increase of particle volume fraction. For  $\text{TiO}_2$ — $\varnothing 15 \text{ nm}$ , the viscosity was  $1.83 \times 10^{-3} \text{ Pa.s}$ , which was observed to increase more significantly with volume fraction compared with  $\text{TiO}_2$ — $\varnothing 10 \text{ nm} \times 40 \text{ nm}$ . This is because of the smaller particle size, shape, and larger number of particles. The pH values of  $\text{TiO}_2$ —deionized water nanofluids are found to be within 6.8–6.2 for the particle volume fraction of 0.001–0.02, which shows that the nanofluid is nearly neutral in nature and it decreases with increasing particle volume fraction. According to Xie et al. [12], the hydration forces among particles increase with a decrease in the pH value of the suspension, which results in the enhanced mobility of nanoparticles in the suspension leading the heat transport process. Hence, the pH value of the nanofluids should be kept low for better heat transport.

### 3. Measurement of thermal conductivity of nanofluids

The transient hot-wire (THW) method is employed to measure the thermal conductivity of sample nanofluids. The measuring principle of the transient hot-wire technique is based on the calculation of the transient temperature field around a thin wire (called hot-wire), which can be treated as a line source. A constant current is supplied to the wire to generate the necessary temperature rise. The wire is surrounded by a sample nanofluid, whose thermal conductivity and thermal diffusivity are to be measured. The wire serves as both the heat source and the temperature sensor. The heat dissipated in the wire increases the temperature of the wire and also that of the sample. The temperature rise in the wire depends on the thermal conductivity of the sample through which the wire is inserted.

#### 3.1. Theoretical basis

The transient hot-wire method is well documented in the literature [13–15]. Thus, the basic assumptions and derivations for the mathematical formulation of the transient hot-wire system are not discussed in detail.

The governing equation for radial transient heat conduction in a homogeneous and infinite medium is given by

$$\frac{\partial^2 \theta}{\partial r^2} + \frac{1}{r} \frac{\partial \theta}{\partial r} = \frac{1}{\alpha} \frac{\partial \theta}{\partial t} \quad (1)$$

where  $\theta = T - T_0$  is the temperature rise in the medium and  $T_0$  is the initial temperature,  $T$  is the temperature in surrounding medium at time  $t$  and radial position  $r$ , and  $\alpha = \frac{k}{\rho c_p}$  is the thermal diffusivity of the surrounding medium.

The initial and outer boundary ( $r \rightarrow \infty$ ) conditions are

$$\theta(r, t) = 0 \quad (2)$$

The inner boundary condition at  $r = a$  is

$$q = -2\pi a k \left. \frac{\partial \theta}{\partial r} \right|_{r=a} \quad \text{for } t > 0 \quad (3)$$

The solution of Eq. (1) for the temperature rise of the hot-wire is obtained as

$$\theta(a, t) = \frac{q}{4\pi k} \left[ \ln t + \ln \frac{4\alpha}{a^2 C} \right] \quad (4)$$

where  $C = \exp(\gamma)$  and  $\gamma = 0.5772$  is Euler's constant.

From Eq. (4), the thermal conductivity of nanofluids can be calculated using the linear relationship between the temperature rise and the natural logarithm of time.

#### 3.2. Mathematical formulation for experiments

From the analogy of the Wheatstone bridge circuit used in the hot-wire apparatus and imposing the mathematical formulation for temperature rise of the hot-wire (Eq. (4)), an integrated mathematical formulation is established for measuring the thermal conductivity and thermal diffusivity simultaneously and more conveniently.

Applying Kirchoff's voltage law to the balanced Wheatstone bridge circuit (Fig. 3) and using the temperature-resistance relationship of wire, the voltage change is given by

$$V_g = \left[ \frac{R_3}{(R_3 + R_w)^2} \right] (\beta R_w) V_s \theta \quad (5)$$

Substituting Eq. (4) into Eq. (5), we have

$$V_g = \left[ \frac{R_3}{(R_3 + R_w)^2} \right] (\beta R_w) \frac{V_s q}{4\pi k} \left[ \ln t + \ln \frac{4\alpha}{a^2 C} \right] \quad (6)$$

For

$$\left[ \frac{\beta R_3 R_w V_s}{(R_3 + R_w)^2} \right] \frac{q}{4\pi k} = A$$

and

$$A \ln \frac{4\alpha}{a^2 C} = B$$

Eq. (6) can be written as the simplest form of

$$V_g = A \ln t + B \quad (7)$$

Since  $V_g$  can be obtained directly from the Wheatstone bridge circuit through the  $A/D$  converter or digital voltmeter, the thermal conductivity and thermal diffusivity can be calculated more conveniently from slope ( $A$ ) and intercept ( $B$ ) of Eq. (7).

#### 3.3. Transient hot-wire apparatus and procedure

The transient hot-wire method has been proved to be one of the most accurate and fast ways of determining the thermal conductivity of a fluid. The advantage of the method lies in its almost complete elimination of the effects of natural convection, whose unwanted presence causes problems

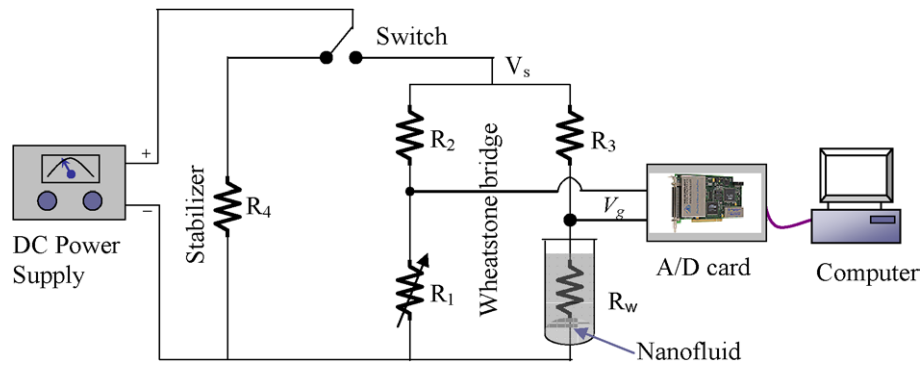


Fig. 3. Schematic of experimental setup.

for measurement. A schematic of the transient hot-wire apparatus used in this study is shown in Fig. 3. The main experimental cell is actually a part of the Wheatstone bridge circuit since the wire (so-called hot-wire) is used as one arm of the bridge circuit. Since these nanofluids are electrically conductive, teflon spray was used for easy and convenient coating of the platinum wire to act as an electric insulation. A bare wire can be used if the fluid is electrically nonconductive. A platinum wire was chosen because of its well-known resistance/temperature relationship over a wide temperature range. The resistance-temperature coefficient of Pt wire is  $0.0039092\text{ }^{\circ}\text{C}^{-1}$  [16]. A thermocouple platinum wire of  $76.2\text{ }\mu\text{m}$  and length of  $215\text{ mm}$  is used in the hot-wire cell whose electric resistance is measured and calculated. It was desired to have a wire with as small a diameter as possible for it to act as a line heat source. For this cell, the wire length to diameter ratio is 2821. The dimensions of the sample container were chosen to be sufficiently large for it to be considered as infinite compared to the platinum wire. The volume capacity and diameter of the sample container are  $80\text{ mL}$  and  $20\text{ mm}$ , respectively.

After calibration, the nanofluids were taken into the hot-wire cell to measure the thermal conductivity. Measurements were performed at room temperature and atmospheric pressure. Initially, the Wheatstone bridge circuit was balanced by adjusting the adjustable resistance in circuit and ground resistance of the analog to digital (A/D) converter input panel. When no voltage change reading was observed (i.e.,  $V_{\text{out}} = 0$ ) in A/D converter, the circuit was considered as balanced. After switching on the DC supply through the stabilizer ( $R_4$ , in Fig. 3) to the Wheatstone bridge circuit, a voltage change occurred in the hot-wire, which caused the circuit to be unbalanced. This unbalanced voltage ( $V_g$ ) over time was recorded in the computer by the A/D converter at a sampling rate of 15 samples/second. Labview software was used to support the A/D converter to obtain the data in required format. The input voltage to the circuit was also recorded for each run. This measured unbalanced voltage over natural logarithm of time was plotted. The thermal conductivity was then calculated from the slope of linear fitted curve. Since this magnitude of slope of fitted curve is equal to the slope of the integrated mathematical linear equation

(Eq. (7)), the thermal conductivity can be easily calculated from the other known parameters.

## 4. Results and discussion

### 4.1. Calibration and error estimation

To estimate the error in measurement of the thermal conductivity, the experimental apparatus was calibrated with a base fluid (deionized water) for different input voltages. For the calibration and experimental operation, each sample result is the average of 1000 scans by the A/D converter. At the same operating condition, the thermal conductivity was determined for each sample and the average is taken. The hot-wire cell was insulated thermally by self-adhesive insulation foam tape to maintain uniform room temperature in an air-conditioned laboratory. The measurements were performed with different input voltages and then a suitable voltage was chosen for each test sample. The time of each run was kept within three seconds to avoid the convection effect. The thermal conductivities of nanofluids were measured in several runs to obtain the statistical standard deviation and the repeatability, which are shown in Fig. 4 as error bars. The standard thermal conductivity of deionized water is considered as  $0.607\text{ W}\cdot\text{m}^{-1}\cdot\text{K}^{-1}$ . Based on the deviation between this standard thermal conductivity of deionized water and the measured thermal conductivity in calibration operation, the measurement error was estimated to be within 2%.

### 4.2. Experimental results

$\text{TiO}_2$  nanoparticles of  $\varnothing 10\text{ nm} \times 40\text{ nm}$  and  $\varnothing 15\text{ nm}$  in deionized water with different volume fractions (0.005–0.05) were tested to measure the thermal conductivity. Both the experimental results (Fig. 4) and the theoretical prediction by various existing models (Figs. 5 and 6) show that the thermal conductivity of  $\text{TiO}_2$ —deionized water based nanofluids increases with particle volume fraction. Fig. 4 shows that the measured thermal conductivity for  $\text{TiO}_2$  ( $\varnothing 15\text{ nm}$ )—water nanofluids has a maximum enhancement 29.70% for a particle volume fraction of 5%. For  $\text{TiO}_2$

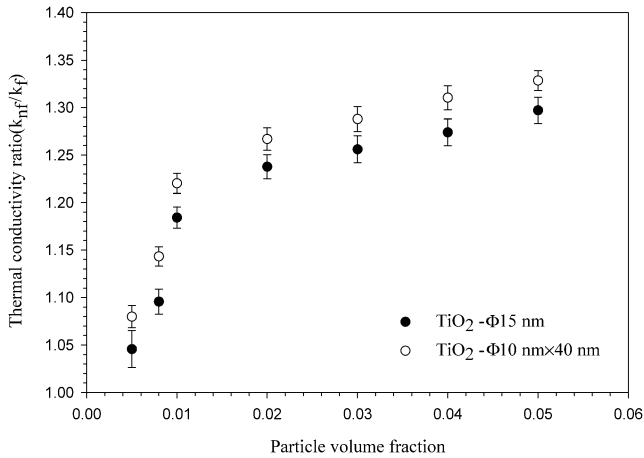


Fig. 4. Enhancement of thermal conductivity of TiO<sub>2</sub>—deionized water nanofluids with CTAB surfactant.

(∅10 nm × 40 nm)—water nanofluids, the maximum enhancement is 32.80% from the base fluid with the same particle volume fraction. The experimental results show a nonlinear relationship between the thermal conductivity and particle volume fraction at lower volumetric loading (0.005–0.02) and a linear relationship at higher volumetric loading (0.02–0.05). This nonlinear behavior of nanofluids at lower volume fractions of nanoparticles may be due to the influence of the CTAB surfactant, long time (8–10 hours) of sonication, and hydrophobic surface forces in the nanofluids. However, the results are in good agreement with those of other researchers [4–10,17], i.e., the thermal conductivities of nanofluids increase as particle volume fraction increases.

It is also observed that for the nanofluid with rod-shape (∅10 nm × 40 nm) nanoparticles, the increase in thermal conductivity is larger than that of the nanofluid with spherical shape (∅15 nm) particles. According to the Hamilton and Crosser model (Eq. (8)), the shape factor ( $n = 6$ ) for cylindrical particles is larger than that for spherical particles with shape factor,  $n = 3$ . This model also shows that the thermal conductivity for the mixture with cylindrical particles is higher than that of the mixture with spherical particles. Due to the larger shape factor, the thermal conductivity of nanofluids composed of rod-shape nanoparticles is larger than that of the nanofluids with spherical shape nanoparticles.

#### 4.3. Comparisons of experimental results with theoretical prediction

Since no exact theory for the determination of thermal conductivity of nanofluids is available as yet, existing classical models for the solid–liquid mixture are used to compare with the measured thermal conductivity. The Maxwell model [18] is used for determining the thermal conductivity of suspensions containing spherical particles. However, thermal conductivity of suspensions depends not only on the particle volume fraction but also on the size and shape of the suspended particles. The results are compared in Figs. 5

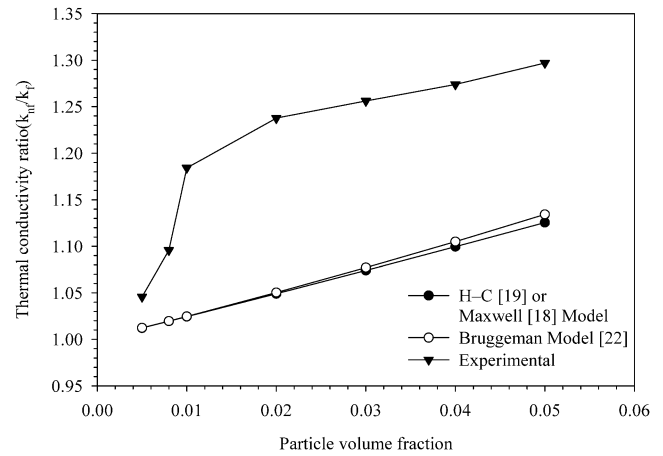


Fig. 5. Comparison between experimental and theoretically determined thermal conductivity of TiO<sub>2</sub> (∅15 nm)—deionized water nanofluids with CTAB surfactant.

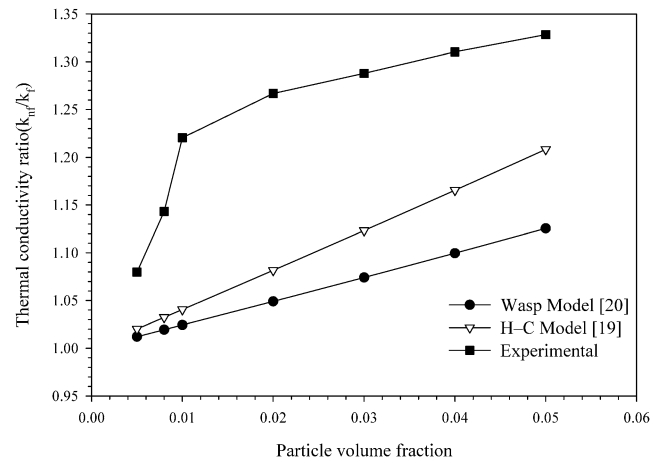


Fig. 6. Comparison between experimental and theoretically determined thermal conductivity of TiO<sub>2</sub> (∅10 nm × 40 nm)—deionized water nanofluids with CTAB surfactant.

and 6 with the theoretical predictions by the model of Hamilton and Crosser (Eq. (8)), Wasp (Eq. (9)), and Bruggeman (Eq. (10)).

The Hamilton and Crosser [19] model for determining the effective thermal conductivity of a two-phase mixture is given by

$$k_{\text{eff}}/k_f = \left[ \frac{k_p + (n - 1)k_f - (n - 1)\phi(k_f - k_p)}{k_p + (n - 1)k_f + \phi(k_f - k_p)} \right] \quad (8)$$

where  $n$  is the empirical shape factor given by  $n = 3/\psi$  and  $\psi$  is the sphericity. For the spherical and cylindrical shape particle, the sphericity ( $\psi$ ) is 1 and 0.5, respectively.

The Wasp model for calculating the effective thermal conductivity of solid–liquid mixtures is given by Xuan and Roetzel [20] and Wang et al. [21] as

$$k_{\text{eff}}/k_f = \frac{k_p + 2k_f - 2\phi(k_f - k_p)}{k_p + 2k_f + \phi(k_f - k_p)} \quad (9)$$

For only spherical particles, the Wasp model yields the same results as the Maxwell and the Hamilton and Crosser models.

The Bruggeman model gives a slightly better prediction [22,23] than other models in the case of spherical particles with no limitations on the concentration of inclusions. It was used to consider the effect of nanoparticle clustering in [23].

For a binary mixture of homogeneous spherical inclusions, the Bruggeman model has

$$k_{\text{eff}} = \frac{1}{4} [(3\phi - 1)k_p + (2 - 3\phi)k_f] + \frac{k_f}{4} \sqrt{\Delta} \quad (10)$$

$$\Delta = [(3\phi - 1)^2 (k_p/k_f)^2 + (2 - 3\phi)^2 + 2(2 + 9\phi - 9\phi^2)(k_p/k_f)] \quad (11)$$

where  $k_{\text{eff}}$  is the effective thermal conductivity of liquid with particle suspension,  $\phi$  is the volume fraction of particles, and  $k_f$  and  $k_p$  are the thermal conductivities of the base fluid and the particle, respectively.

For  $\text{TiO}_2$  ( $\varnothing 15$  nm) nanofluids, it can be seen from Fig. 5 that the experimental thermal conductivity is about 17% higher than the theoretical predictions by the Hamilton–Crosser and Bruggeman models for a sample of 5% nanoparticles in deionized water. By considering interactions between randomly distributed particles, the Bruggeman model shows a better prediction than that of the H–C or Maxwell models. Fig. 6 shows that the experimentally measured thermal conductivity for  $\text{TiO}_2$  ( $\varnothing 10$  nm  $\times$  40 nm)—deionized water nanofluids is at most 12% higher than that predicted by H–C model. By accounting for the shape of the particles, the H–C model gives a better prediction than that of the Wasp model for the effective thermal conductivity of a mixture.

From the comparison of our experimental results and the theoretical predictions by these traditional models, it is observed that all these models underpredict the effective thermal conductivity of nanofluids. This is probably because these traditional models do not account for particle size, particle Brownian motion, nanolayering, and effect of nanoparticles clustering [5], which are important to nanoparticles in nanofluids [24].

## 5. Conclusions

Since nanoparticles cannot be expected to be well dispersed in their base fluids, surfactants can play an effective role for proper dispersion of nanoparticles to ensure higher heat transfer performance of nanofluids. An integrated correlation model was introduced to allow a more precise and convenient determination of the thermal conductivity of nanofluids by the transient hot-wire method. The experimental results show that nanofluids containing a small amount of nanoparticles have much higher thermal conductivities than normal base fluids. The thermal conductivity of nanofluids increases remarkably with increasing volume fraction of nanoparticles. Particle size and shape also influence the

thermal conductivity enhancement of nanofluids. The experimental results are compared with theoretical predictions by several existing models. It is found that the experimental results are remarkably higher than those predicted by existing models for solid–liquid mixtures. The comparisons indicate that further research efforts are needed to develop a suitable model to predict the thermal conductivity of nanofluids which will take into account several possible factors in enhancing the heat transfer performance of nanofluids.

## References

- [1] S.U.S. Choi, Enhancing thermal conductivity of fluids with nanoparticles, in: D.A. Siginer, H.P. Wang (Eds.), *Developments and Applications of Non-Newtonian Flows*, in: FED, vol. 231/MD, vol. 66, ASME, New York, 1995, pp. 99–103.
- [2] S. Zussman, More about Argonne's stable, highly conductive nanofluids, Technology Transfer at Argonne, Public communication, Argonne National Laboratory, IL, USA, 2002.
- [3] J.A. Eastman, S.R. Phillpot, S.U.S. Choi, P. Keblinski, Thermal transport in nanofluids, *Annual Rev. Mater. Res.* 34 (2004) 219–246.
- [4] S.K. Das, N. Putra, P. Thiesen, W. Roetzel, Temperature dependence of thermal conductivity enhancement for nanofluids, *J. Heat Transfer* 125 (2003) 567–574.
- [5] Y. Xuan, Q. Li, W. Hu, Aggregation structure and thermal conductivity of nanofluids, *AIChE J.* 49 (2003) 1038–1043.
- [6] J.A. Eastman, S.U.S. Choi, S. Li, L.J. Thompson, Enhanced thermal conductivity through the development of nanofluids, in: *Proceedings of the Symposium on Nanophase and Nanocomposite Materials II*, vol. 457, Materials Research Society, Boston, 1997, pp. 3–11.
- [7] J.A. Eastman, S.U.S. Choi, S. Li, W. Yu, L.J. Thompson, Anomalous increased effective thermal conductivities of ethylene glycol-based nanofluids containing copper nanoparticles, *Appl. Phys. Lett.* 78 (2001) 718–720.
- [8] S. Lee, S.U.S. Choi, S. Li, J.A. Eastman, Measuring thermal conductivity of fluids containing oxide nanoparticles, *J. Heat Transfer* 121 (1999) 280–289.
- [9] X. Wang, X. Xu, S.U.S. Choi, Thermal conductivity of nanoparticle–fluid mixture, *J. Thermophys. Heat Transfer* 13 (1999) 474–480.
- [10] Y. Xuan, Q. Li, Heat transfer enhancement of nanofluids, *Internat. J. Heat Fluid Flow* 21 (2000) 58–64.
- [11] M. Sakamoto, Y. Kanda, M. Miyahara, K. Higashitani, Origin of long-range attractive force between surfaces hydrophobized by surfactant adsorption, *Langmuir* 18 (2002) 5713–5719.
- [12] H. Xie, J. Wang, T. Xi, Y. Liu, F. Ai, Thermal conductivity enhancement of suspensions containing nanosized alumina particles, *J. Appl. Phys.* 91 (2002) 4568–4572.
- [13] J.W. Haarman, A contribution to the theory of the transient hot-wire method, *Physica* 52 (1971) 605–619.
- [14] J.J. Healy, J.J. de Groot, J. Kestin, The theory of the transient hot-wire method for measuring thermal conductivity, *Physica C* 82 (1976) 392–408.
- [15] Y. Nagasaka, A. Nagashima, Absolute measurement of the thermal conductivity of electrically conducting liquids by the transient hot-wire method, *J. Phys. E: Sci. Instrum.* 14 (1981) 1435–1440.
- [16] J.P. Bentley, Temperature sensor characteristics and measurement system design, *J. Phys. E: Sci. Instrum.* 17 (1984) 430–439.
- [17] Y. Wang, T.S. Fisher, J.L. Davidson, L. Jiang, Thermal conductivity of nanoparticle suspensions, in: *Proceedings of 8th AIAA/ASME Joint Thermophysics and Heat Transfer Conference*, AIAA 2002-3345, Missouri, 2002, pp. 1–6.
- [18] J.C. Maxwell, *A Treatise on Electricity and Magnetism*, third ed., Clarendon Press, Oxford, 1891.
- [19] R.L. Hamilton, O.K. Crosser, Thermal conductivity of heterogeneous two component systems, *I & EC Fundamentals* 1 (1962) 187–191.

- [20] Y. Xuan, W. Roetzel, Conceptions for heat transfer correlation of nanofluid, *Internat. J. Heat Mass Transfer* 43 (2000) 3701–3707.
- [21] B.-X. Wang, H. Li, X.F. Peng, Research on the heat-conduction enhancement for liquid with nano-particle suspensions, General Paper (G-1), International Symposium on Thermal Science and Engineering (TSE2002), Beijing, 2002.
- [22] Y. Ding, D. Wen, R.A. Williams, Nanofluids for heat transfer intensification—where are we and where should we go?, in: Proceedings of 6th International Symposium on Heat Transfer, Beijing, 2004, pp. 66–76.
- [23] B.-X. Wang, L.-P. Zhou, X.-P. Peng, A fractal model for predicting the effective thermal conductivity of liquid with suspension of nanoparticles, *Internat. J. Heat Mass Transfer* 46 (2003) 2665–2672.
- [24] S.U.S. Choi, X. Xu, P. Keblinski, W. Yu, Nanofluids can take the heat, in: DOE BES 20th Symposium on Energy Engineering Sciences, Argonne, USA, 2002.